Calcium carbonate budget in the Atlantic Ocean based on water column inorganic carbon chemistry

S.-N. Chung,[1] K. Lee,[1] R. A. Feely,[2] C. L. Sabine,[2] F. J. Millero,[3] R. Wanninkhof,[4] J. L. Bullister,[2] R. M. Key,[5] and T.-H. Peng[4]

Received 25 October 2002; revised 21 June 2003; accepted 25 July 2003; published 9 October 2003.

[1] Recent independent lines of evidence suggest that the dissolution of calcium carbonate ($CaCO_3$) particles is substantial in the upper ocean above the calcite 100% saturation horizon. This shallow-water dissolution of carbonate particles is in contrast with the current paradigm of the conservative nature of pelagic $CaCO_3$ at shallow water depths. Here we use more than 20,000 sets of carbon measurements in conjunction with CFC and ^{14}C data from the WOCE/JGOFS/OACES global CO_2 survey to estimate in situ dissolution rates of $CaCO_3$ in the Atlantic Ocean. A dissolution rate is estimated from changes in alkalinity as a parcel of water ages along an isopycnal surface. The in situ $CaCO_3$ dissolution increases rapidly at the aragonite 100% saturation horizon. Estimated dissolution rates north of 40°N are generally higher than the rates to the south, which is partly attributable to the production of exported $CaCO_3$ being higher in the North Atlantic than in the South Atlantic. As more $CaCO_3$ particles move down the water column, more particles are available for in situ dissolution. The total water column $CaCO_3$ dissolution rate in the Atlantic Ocean is determined on an annual basis by integrating estimated dissolution rates throughout the entire water column and correcting for alkalinity input of approximately 5.6×10^{12} mol C yr^{-1} from $CaCO_3$-rich sediments. The resulting water column dissolution rate of $CaCO_3$ for the Atlantic Ocean is approximately 11.1×10^{12} mol C yr^{-1}. This corresponds to about 31% of a recent estimate (35.8×10^{12} mol C yr^{-1}) of net $CaCO_3$ production by *Lee* [2001] for the same area. Our calculation using a large amount of high-quality water column alkalinity data provides the first basin-scale estimate of the $CaCO_3$ budget for the Atlantic Ocean. *INDEX TERMS:* 4805 Oceanography: Biological and Chemical: Biogeochemical cycles (1615); 4806 Oceanography: Biological and Chemical: Carbon cycling; 4835 Oceanography: Biological and Chemical: Inorganic marine chemistry; 4825 Oceanography: Biological and Chemical: Geochemistry; *KEYWORDS:* calcium carbonate budget, dissolution of calcium carbonate, alkalinity, ocean carbon cycle, saturation state of seawater

Citation: Chung, S.-N., K. Lee, R. A. Feely, C. L. Sabine, F. J. Millero, R. Wanninkhof, J. L. Bullister, R. M. Key, and T.-H. Peng, Calcium carbonate budget in the Atlantic Ocean based on water column inorganic carbon chemistry, *Global Biogeochem. Cycles*, *17*(4), 1093, doi:10.1029/2002GB002001, 2003.

1. Introduction

[2] The marine carbonate system affects the long-term fate of anthropogenic CO_2 in the oceans and the rate of atmospheric CO_2 increase by controlling the rate of oceanic CO_2 uptake. Therefore many studies have focused on the fundamental processes controlling the distribution of the four inorganic CO_2-system parameters in the oceans: fugacity of CO_2 (fCO_2), total dissolved inorganic carbon (C_T), total alkalinity (TA), and pH ($-\log_{10}[H^+]$). Knowledge of the rate of CO_2 removal from the surface ocean via biogenic $CaCO_3$ and of the ultimate delivery rate of $CaCO_3$ to regions of the deep ocean that are corrosive to $CaCO_3$ particles is incomplete. Since the settling time of $CaCO_3$ particles is thought to be short compared to dissolution rates, it was generally believed that much of the carbonate dissolution takes place on or just beneath the surface of the sediments. However, evidence from a variety of sources suggests that as much as 60–80% of net $CaCO_3$ production is dissolved in depths that are above the chemical lysocline,

[1]School of Environmental Science and Engineering, Pohang University of Science and Technology, Pohang, Republic of Korea.
[2]Pacific Marine Environmental Laboratory, NOAA, Seattle, Washington, USA.
[3]Rosenstiel School of Marine and Atmospheric Studies, University of Miami, Miami, Florida, USA.
[4]Atlantic Oceanographic and Meteorological Laboratory, NOAA, Miami, Florida, USA.
[5]Atmospheric and Oceanic Sciences Program, Princeton University, Princeton, New Jersey, USA.

0886-6236/03/2002GB002001$12.00

the depth below which the rate of $CaCO_3$ dissolution distinctly increases [*Milliman et al.*, 1999; *François et al.*, 2002].

[3] It is well known that >80% of sinking organic matter is oxidized within the upper 1000–2000 m of the water column [*Lutz et al.*, 2002], but much less is known about the amount of $CaCO_3$ that dissolves in the water column and about the underlying processes. The biological production and dissolution of $CaCO_3$ in the ocean result in changes in TA in the water column according to the following reaction:

$$CaCO_3 + H_2O + CO_2 \leftrightarrow Ca^{2+} + 2HCO_3^- . \quad (1)$$

A change in the balance of this reaction in the ocean would have a significant impact on atmospheric CO_2 concentration [*Zondervan et al.*, 2001]. Dissolution of $CaCO_3$ particles increases TA in seawater and thus the capacity of the ocean to absorb CO_2 from the atmosphere, whereas the production of $CaCO_3$ leads to the opposite consequence.

[4] Two papers published in 1984 provide substantial evidence that the dissolution of aragonite occurs in the upper waters (where the depth is <1000 m) of the Pacific Ocean [*Betzer et al.*, 1984; *Byrne et al.*, 1984]. *Milliman et al.* [1999] also presented several independent lines of evidence supporting the dissolution of $CaCO_3$ particles in the upper 1000 m of the water column. If this upper-water dissolution of $CaCO_3$ is significant, we may need to modify the long-held paradigm of the conservative nature of pelagic $CaCO_3$ at upper water depths. In this paper, we use data from the World Ocean Circulation Experiment/Joint Global Ocean Flux Study/Ocean Atmosphere Carbon Exchange Study (WOCE/JGOFS/OACES) CO_2 survey of the Atlantic Ocean to estimate in situ dissolution rates of $CaCO_3$ in the water column by examining changes in TA along isopycnal surfaces. We also provide a $CaCO_3$ budget for the Atlantic Ocean using the net $CaCO_3$ production from *Lee* [2001], the water column dissolution of $CaCO_3$, and the dissolution of $CaCO_3$ from sediments. This paper, in conjunction with the analyses of *Feely et al.* [2002] for the Pacific Ocean and *Sabine et al.* [2002a] for the Indian Ocean, provides a first look at the global $CaCO_3$ budget based on water column TA distribution.

2. Source of Data and Calculation Methods

2.1. WOCE/JGOFS/OACES Data

[5] Most of the carbon measurements used in this study were collected as part of the WOCE/JGOFS/OACES Atlantic survey between 1990 and 1998 (Figure 1). A total of 23 U.S. and European cruises were included in this analysis. TA values calculated from C_T–pH or C_T–fCO_2 using thermodynamic constants were also included in this dataset when measured TA values were not available. The carbonic acid dissociation constants of *Mehrbach et al.* [1973] as refitted by *Dickson and Millero* [1987] were used in this calculation. Data from different sources were compiled, and the consistency of inorganic carbon measurements (fCO_2, C_T, TA, and pH) made on different cruises was quality checked following the procedures used by *Lamb et al.* [2002]. The consistency checks for the Atlantic data focused on C_T and TA, because these parameters are used in the calculation of anthropogenic CO_2 concentrations and in large-scale biogeochemical carbon cycling studies.

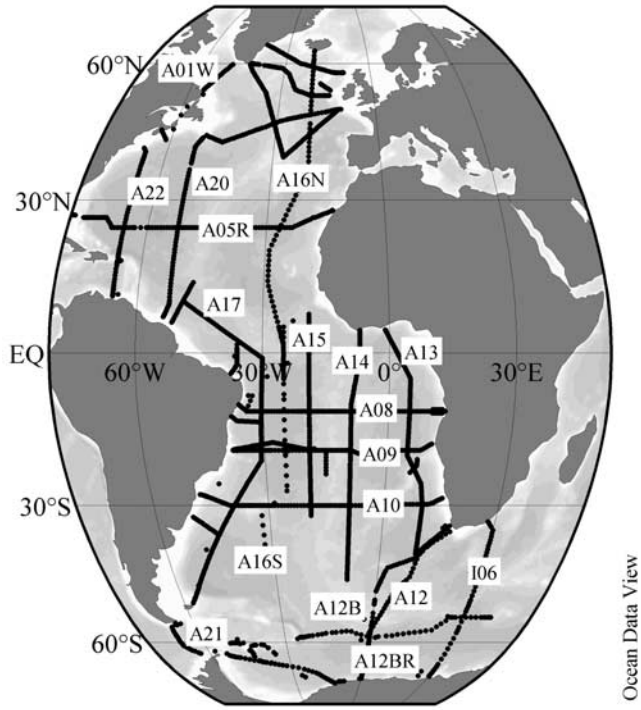

Figure 1. Locations of data used in the analyses. These data were collected as part of the World Ocean Circulation Experiment (WOCE) hydrographic program, the Joint Global Ocean Flux Studies (JGOFS), and the Ocean–Atmosphere Carbon Exchange Study (OACES) of the National Oceanic and Atmospheric Administration (NOAA) between 1990 and 1998. The cruise designations follow the WOCE nomenclature.

[6] Four independent methods were used to determine if there were systematic offsets between the various cruises: (1) Inorganic carbon-system values in deep water were compared where cruise tracks crossed, which are referred to as ''crossover analyses''; (2) multiparameter linear regressions of C_T (or TA) with potential temperature, salinity, oxygen, silicate, and nitrate were created for cruises that followed the same cruise track, and the calculated values were then compared with the measured parameters for individual cruises; (3) on cruises where more than two carbon-system parameters were measured, the internal consistency between parameters was determined from known thermodynamic relationships between the parameters; and (4) regional multiparameter linear regressions of C_T (or TA) with potential temperature, salinity, oxygen, silicate, and phosphate were created using data that were deemed accurate based on the previous checks. The C_T and TA values calculated from the regressions were then compared with individual cruises that showed significant offsets in the crossover analysis. These analyses suggest that the systematic cruise-to-cruise differences for C_T and TA are small except for two cruises [*Wanninkhof et al.*, 2003]. Adjustments of +14 and −7 μmol kg^{-1} were recommended for TA values on

A01W and A09, respectively, whereas no specific adjustments for C_T were required. After adjusting the A01W and A09 TA data, the entire data set is believed to be internally consistent to ±4 and ±6 μmol kg^{-1} for C_T and TA, respectively. The final data set comprises 28,639 measurements of C_T and 18,771 measurements of TA, and is available at http://cdiac.ornl.gov/oceans/datameta.html.

[7] Various tests were also carried out to evaluate the quality of the chlorofluorocarbon (CFC) data, including comparing air measurements with global atmospheric CFC trends [*Walker et al.*, 2000] and with surface CFC concentration measurements, and examining the consistency of CFC concentration and CFC-11/CFC-12 ratio measurements along vertical profiles. CFC concentration and ratio measurements were also compared along sections and at crossover stations. A data-quality flag was assigned to each CFC measurement based on WOCE guidelines, and the CFC data are reported as picomole per kilogram seawater on the SIO98 calibration scale. These data are available at http://cdiac.ornl.gov/oceans/datameta.html.

2.2. Seawater TA

[8] The TA of seawater is defined as the number of moles of hydrogen ions equivalent to the excess of proton acceptors (bases formed from weak acids with $pK \geq 4.5$ at 25°C and zero ionic strength) over proton donors (acids with $pK < 4.5$) in 1 kg of sample [*Dickson*, 1981],

$$\begin{aligned} TA = &[HCO_3^-] + 2[CO_3^{2-}] + [B(OH)_4^-] + [OH^-] \\ &+ [HPO_4^{2-}] + 2[PO_4^{3-}] + [SiO(OH)_3^-] \\ &- [H^+]_F - [HSO_4^-] - [HF] - [H_3PO_4], \end{aligned} \quad (2)$$

where brackets represent concentrations in seawater (μmol kg^{-1}) and $[H^+]_F$ is the concentration of free hydrogen ions. The concentrations of NH_3 and HS^- are not included in equation (2) because they are generally very low in open-ocean water.

[9] The dominant processes that modify surface-seawater TA are evaporation and fresh-water inputs, which manifest themselves as variations in salinity. In deep waters, where salinity variations are considerably smaller, the formation or dissolution of biogenic $CaCO_3$ becomes important in determining the variations in TA. The net addition of carbonate ion (CO_3^{2-}) increases seawater TA, whereas the release of protons during the remineralization of organic matter decreases seawater TA (this latter process is less significant). Thus the latter two processes result in a compensatory effect on the change in TA, and so the change in measured TA in a particular water parcel provides a lower limit on the amount of $CaCO_3$ that dissolves. However, in our work the release of protons by organic matter remineralization is corrected for in the calculation by assuming a constant stoichiometric ratio between dissolution and organic remineralization (see equation (6) in section 2.4).

2.3. Saturation State of Seawater With Respect to Calcium Carbonate

[10] Most of the upper water is supersaturated with aragonite and calcite, while much of the deep water is undersaturated. The degree of saturation of seawater with aragonite or calcite is defined as the ratio of the ion product of the concentrations of calcium ($[Ca^{2+}]$) and $[CO_3^{2-}]$ at the in situ temperature, salinity, and pressure, divided by the stoichiometric solubility product with respect to aragonite (*K*sp-arg*) and calcite (*K*sp-cal*) at the same conditions,

$$\Omega\text{arg} = [Ca^{2+}][CO_3^{2-}]/K^*sp\text{–}arg \quad (3)$$

$$\Omega\text{cal} = [Ca^{2+}][CO_3^{2-}]/K^*sp\text{–}cal. \quad (4)$$

[11] The values of *K*sp-arg* and *K*sp-cal* at 1 atmosphere as a function of temperature and salinity were determined by *Mucci* [1983]. The effect of pressure on the solubility of aragonite or calcite was estimated from the measurements of *Ingle* [1975]. When $\Omega > 1$, seawater is supersaturated with respect to aragonite (or calcite); conversely, when $\Omega < 1$, seawater is undersaturated. Since the calcium-to-salinity ratio in seawater does not vary by more than ~1.5%, variations in the ratio of $[CO_3^{2-}]$ to the stoichiometric solubility product primarily govern the degree of saturation of seawater with respect to aragonite or calcite. In situ $[CO_3^{2-}]$ in seawater was calculated from a pair of measured inorganic carbon parameters (e.g., TA + C_T, or pCO_2 + C_T) using the set of pressure-corrected thermodynamic constants, which was previously shown to be the most consistent with a calibrated field dataset compiled from a global carbon survey [*Lee et al.*, 2000]. The constants we used include the carbonic acid dissociation constants of *Mehrbach et al.* [1973] as refitted by *Dickson and Millero* [1987], along with equilibrium constants of other ancillary components (e.g., boric acid dissociation, solubility of CO_2, water hydrolysis, and phosphoric- and silicic-acid dissociation) necessary to characterize the carbonate system in seawater as summarized by *Millero* [1995]. The pressure effect on these thermodynamic constants was estimated from molal volume and compressibility data [*Millero*, 1983, 1995],

$$\ln\left(K_i^P/K_i^0\right) = -(\Delta V_i/RT)P + (0.5\Delta K_i/RT)P^2, \quad (5)$$

where R is the gas constant, P is the applied pressure, and ΔV_i and ΔK_i are changes in molal volume and compressibility for dissociation constants of various acids. All calculations were made using the QuickBasic CO_2 program developed by K. Lee, which was based on the earlier version by F.J. Millero (University of Miami). Results calculated using this program were the same as those calculated using a CO_2 program developed by *Lewis and Wallace* [1998], which is available at http://cdiac.esd.ornl.gov/oceans/home.html. The concentrations of calcium, borate, sulfate, and fluoride were estimated using the equations of *Riley and Tongudai* [1967], *Uppström* [1974], *Morris and Riley* [1966], and *Riley* [1965], respectively.

[12] We also calculated aragonite and calcite saturation states of seawaters in the preindustrial era using the same program and equations, and measured TA and estimates of preindustrial levels of C_T (C_T°) for all water samples

Table 1. Estimated Errors in the Calculated Values of Ωarg and Ωcal Caused by Uncertainties in Thermodynamic Constants and Measured Parameters[a]

Input Parameters and Uncertainties	Estimated Error of Ωarg (2500 m)
$\Delta K^*sp\text{-}arg = \pm 0.13$[b]	±0.022
Pressure-corrected $\Delta K^*sp\text{-}arg = \pm 0.641$[c]	±0.040
Measured ΔTA and $\Delta C_T = \pm 4$[d] and ±2[e] μmol kg^{-1}	±0.048
$\Delta K_i^* = \pm 0.004$[f]	±0.012
Input Parameters and Uncertainties	**Estimated Error of Ωcal (4500 m)**
$\Delta K^*sp\text{-}cal = \pm 0.16$[b]	±0.069
Pressure-correctedΔ $K^*sp\text{-}cal = \pm 1.084$[c]	±0.070
Measured ΔTA and $\Delta C_T = \pm 4$[d] and ±2[e] μmol kg^{-1}	±0.048
$\Delta K_i^* = \pm 0.004$[f]	±0.018

[a]Probable error for Ωarg: ±0.067; probable error for Ωcal: ±0.11; K_i^*: dissociation constants of carbonic and boric acids.
[b][*Mucci*, 1983].
[c][*Ingle*, 1975].
[d][*Millero et al.*, 1993].
[e][*Johnson et al.*, 1993].
[f][*Millero*, 1995].

taken during the WOCE/JGOFS/OACES Atlantic survey. We assumed in this calculation that TA has not changed due to oceanic uptake of anthropogenic CO_2 during the industrial era. The C_T^o for each sample was obtained by subtracting out the anthropogenic CO_2 concentration (K. Lee et al., An updated anthropogenic CO_2 inventory in the Atlantic Ocean, submitted to *Global Biogeochemical Cycles*, 2003) (hereinafter referred to as Lee et al., submitted manuscript, 2003) using the modified version of the ΔC* approach developed by *Gruber et al.* [1996]. The extension of the method includes the more accurate treatment of nonlinear mixing between the air-sea disequilibria of end-member water types on an isopycnal surface using an optimum multiparameter analysis (for details see *Sabine et al.* [2002b] and Lee et al. (submitted manuscript, 2003)). A preformed TA estimate different from that of *Gruber et al.* [1996] is also used. Our estimation is based on high-quality Atlantic surface (<100 dbar) TA data.

[13] The probable errors in the Ωarg = 1 and Ωcal = 1 saturation horizons due to uncertainties in equilibrium constants and in measured TA and C_T values are given in Table 1. Uncertainties for measured thermodynamic constants were taken from the original works [*Ingle*, 1975; *Mucci*, 1983; *Millero*, 1995], and those for the measured parameters were from *Wanninkhof et al.* [2003]. Estimated probable errors are ±0.067 in Ωarg for water at 2500 m and ±0.11 in Ωcal for water at 4500 m, which equate to uncertainties of ±300 m in the Ωarg = 1 saturation depth and of ±470 m in the Ωcal = 1 saturation depth. The probable error is the square root of the sum of the squared errors due to uncertainties in thermodynamic constants and measured parameters.

2.4. Determination of the In Situ Dissolution Rate of $CaCO_3$

[14] The amount of $CaCO_3$ dissolved in a subsurface water parcel is estimated from changes in TA by subtracting out the preformed TA concentration and correcting for the TA decrease resulting from the release of protons during the remineralization of organic matter. The contribution from organic matter is determined by using apparent oxygen utilization (AOU = O_2 (saturated values at a given temperature and salinity) − O_2 (measured)) as an indicator. These corrections introduce a new tracer ΔTA^{CaCO3} that is used in this paper to quantify the amount of $CaCO_3$ dissolved in the water mass in question,

$$\Delta TA^{CaCO3}\left(\mu mol\ kg^{-1}\right) = 0.5 \times (TA_{MEAS} - TA^{\circ}) + 0.63 \times (0.0941 \times AOU), \quad (6)$$

where TA_{MEAS} is the measured TA, and TA^o is the preformed TA. The second term on the right-hand side accounts for the decrease in TA resulting from the oxidation of organic matter by using AOU, and the N/O_2 ratio(= 0.0941) [*Anderson and Sarmiento*, 1994] is used rather than nitrate concentration to avoid having to directly estimate the preformed nitrate values [*Chen*, 1978]. A coefficient of 0.63 proposed by *Kanamori and Ikegami* [1982] was also used to account for TA contributions from the oxidation of organic nitrogen, phosphorus, and sulfur. This coefficient was derived from the assumption that reduced sulfur in organic matter is completely oxidized to sulfate and that the contribution of resulting sulfate to TA would be about 20% of the total contribution from nitrate and phosphorus. Therefore the coefficient of 0.63 is about 20% higher than a commonly used value of 0.53, which accounts only for the change in TA caused by the oxidation of organic nitrogen and phosphorus. Equation (6) differs slightly from those in the companion papers of *Feely et al.* [2002] and *Sabine et al.* [2002a], in which NTA (NTA = TA × 35/S, where S is the salinity) was used instead of TA. Also, here the term ΔTA^{CaCO3} is used, which is comparable to their TA* term. The results using either TA or NTA are nearly identical for a salinity of 33−37.

[15] The TA° of a water parcel in the interior of the ocean is an estimate of TA that the water had when it was last at the surface. We estimated TA° from a multilinear regression model using conservative tracers such as S and NO as independent variables. NO is defined as $NO = O_2 - R_{O2/N} \times N$ [*Broecker*, 1974]; we used $R_{O2/N} = -10.625$ [*Anderson and Sarmiento*, 1994]. The TA data (<100 dbar) from the WOCE/JGOFS/OACES Atlantic CO_2 survey gave the following relationship:

$$TA^{\circ}\left(\mu molkg^{-1}\right) = 318.3 + 56.27 \times S + 0.09016 \times NO, \quad (7)$$

where S is on the practical salinity scale, and NO is in μmol kg^{-1}. The standard error (1σ) of the estimated TA° is ±10.3 μmol kg^{-1} based on 2345 data points. Only half of this error is reflected in estimating ΔTA^{CaCO3}, because half of the TA change equates to the $CaCO_3$ change. We used NO rather than PO ($PO = O_2 - R_{O2/P} \times P$) because significant data gaps exist in the Atlantic phosphorus data set. The loss of nitrate due to water column denitrification is insignificant in the Atlantic Ocean [*Gruber and Sarmiento*, 1997] and should not affect our calculations. The probable error of the estimated ΔTA^{CaCO3} due to uncertainties in measured and preformed TA and in the

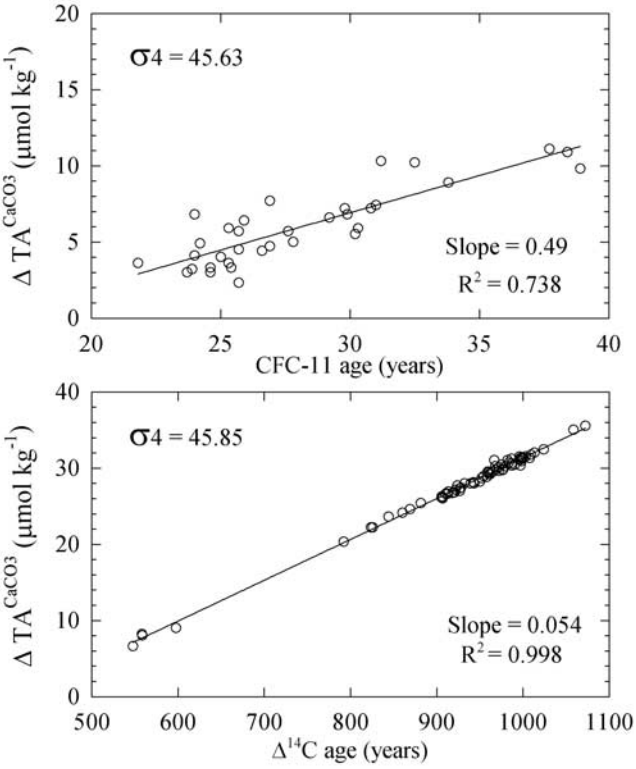

Figure 2. Plots of ΔTA^{CaCO3} versus CFC-11 and $\Delta^{14}C$ ages for data collected along two potential densities in intermediate and deep waters of the North Atlantic.

N/O_2 ratio is ±8 μmol kg^{-1} based on an uncertainty of ±6 μmol kg^{-1} in measured TA [*Wanninkhof et al.*, 2003], of ±10.3 μmol kg^{-1} in preformed TA [see equation (7)], and of ±0.0218 in the N/O_2 ratio [*Anderson and Sarmiento*, 1994].

[16] If $CaCO_3$ dissolution occurs in a given water parcel, values of ΔTA^{CaCO3} increase as the water parcel ages. If the effects of mixing between different water masses are taken into account accurately, the slope between values of ΔTA^{CaCO3} and corresponding ages of water parcels can be used as the in situ dissolution rate of $CaCO_3$ particles (this assumes that changes in ΔTA^{CaCO3} along isopycnal surfaces are solely due to water column dissolution of $CaCO_3$ particles). An alternative method for estimating the dissolution rate is to divide each value of ΔTA^{CaCO3} by its age. However, the rate determined by this method might include a large error if there is systematic age biasing as discussed in section 2.5. Therefore, in this paper we estimated the in situ $CaCO_3$ dissolution on isopycnal surfaces by determining the slope between values of ΔTA^{CaCO3} and ages of water parcels. Systematic age biasing may not significantly affect our slope-based results as long as its magnitude is constant over the period of analysis.

[17] To estimate in situ $CaCO_3$ dissolution rates in waters where values of ΔTA^{CaCO3} are positive, we plotted them against water parcel ages derived from CFC-11 for the upper ocean and ^{14}C for deep waters where CFC-11 is not detected (Figure 2). The CFC-11 age was calculated by converting the CFC-11 concentration (in pmol kg^{-1}) in the subsurface water to partial pressure (*p*CFC-11) at the potential temperature and salinity [*Doney and Bullister*, 1992] and then matching *p*CFC of the subsurface water with the *p*CFC of the atmosphere for the appropriate year. In this calculation, the subsurface water parcel is assumed to have been in solubility equilibrium when it was in contact with the overlying atmospheric *p*CFC-11. Thus the age of the subsurface water is defined as the time difference between the measurement date and the date when the water parcel was last in contact with the atmosphere. The use of CFC-11 age is limited to upper waters with CFC-11 ages less than 35 years (corresponding to ~0.1 pmol kg^{-1}) because systematic biases in CFC ages due to dilution and nonlinear mixing effects tend to be larger for older waters [*Warner et al.*, 1996; *Doney et al.*, 1997; *Sonnerup*, 2001]. Some of the potential uncertainties associated with the use of the tracer to date water masses are discussed further in section 2.5.

[18] For waters with CFC-based ages greater than 35 years, we used age estimates from natural $\Delta^{14}C$. For waters that contained bomb-generated ^{14}C, this was subtracted from the total radiocarbon ($\Delta^{14}C$) to derive the natural $\Delta^{14}C$ component. *Rubin and Key* [2002] proposed a separation method based on the strong correlation between natural $\Delta^{14}C$ and potential alkalinity (*P*TA = (TA + nitrate) × 35/S). We used their *P*TA–$\Delta^{14}C$ algorithm along with *P*TA data calculated from the WOCE/JGOFS/OACES dataset to estimate naturally occurring $\Delta^{14}C$. Resulting estimates of natural $\Delta^{14}C$ were then used to calculate the age of water parcels. The natural $\Delta^{14}C$ is a good method for determining the age of intermediate and deep waters because this isotope has a half-life of 5730 ± 40 years [*Godwin*, 1962]. The use of natural $\Delta^{14}C$ is confined to waters deeper than 1500 m in most of the Atlantic Ocean, except for the northern North Atlantic where the CFC penetrates to waters deeper than 1500 m due to deep convective mixing.

2.5. Uncertainty in Estimated Dissolution Rates

[19] Estimated dissolution rates of $CaCO_3$ are subject to change due to two important sources of errors: (1) the uncertainty in estimating ΔTA^{CaCO3}: we do not estimate dissolution rates if waters have ΔTA^{CaCO3} less than 8 μmol kg^{-1}, which is close to the probable error in estimating ΔTA^{CaCO3}; and (2) the uncertainty in the *p*CFC-based age: the tracer age is not necessarily identical to the true or ideal ventilation age. Because of the nonlinear atmospheric-CFC history, mixing of waters with different *p*CFCs can introduce significant bias in the resulting *p*CFC ages, compared to the true age of the water. Age biasing due to mixing has been examined using observational data and simple models [e.g., *Doney et al.*, 1997; *Sonnerup*, 2001]. Because of the quasi-linear increase in atmospheric CFC-11 during 1965–1990, mixing between waters ventilated during this period should produce relatively small age biases. Age biasing can be significantly greater for mixing between younger and older waters, which tends to bias the age of the mixture toward the younger (higher-CFC-bearing) component. In this study we limit the use of *p*CFC ages for the calculation of $CaCO_3$ dissolution rates to waters with CFC ages <35 years. The rates we obtained might also

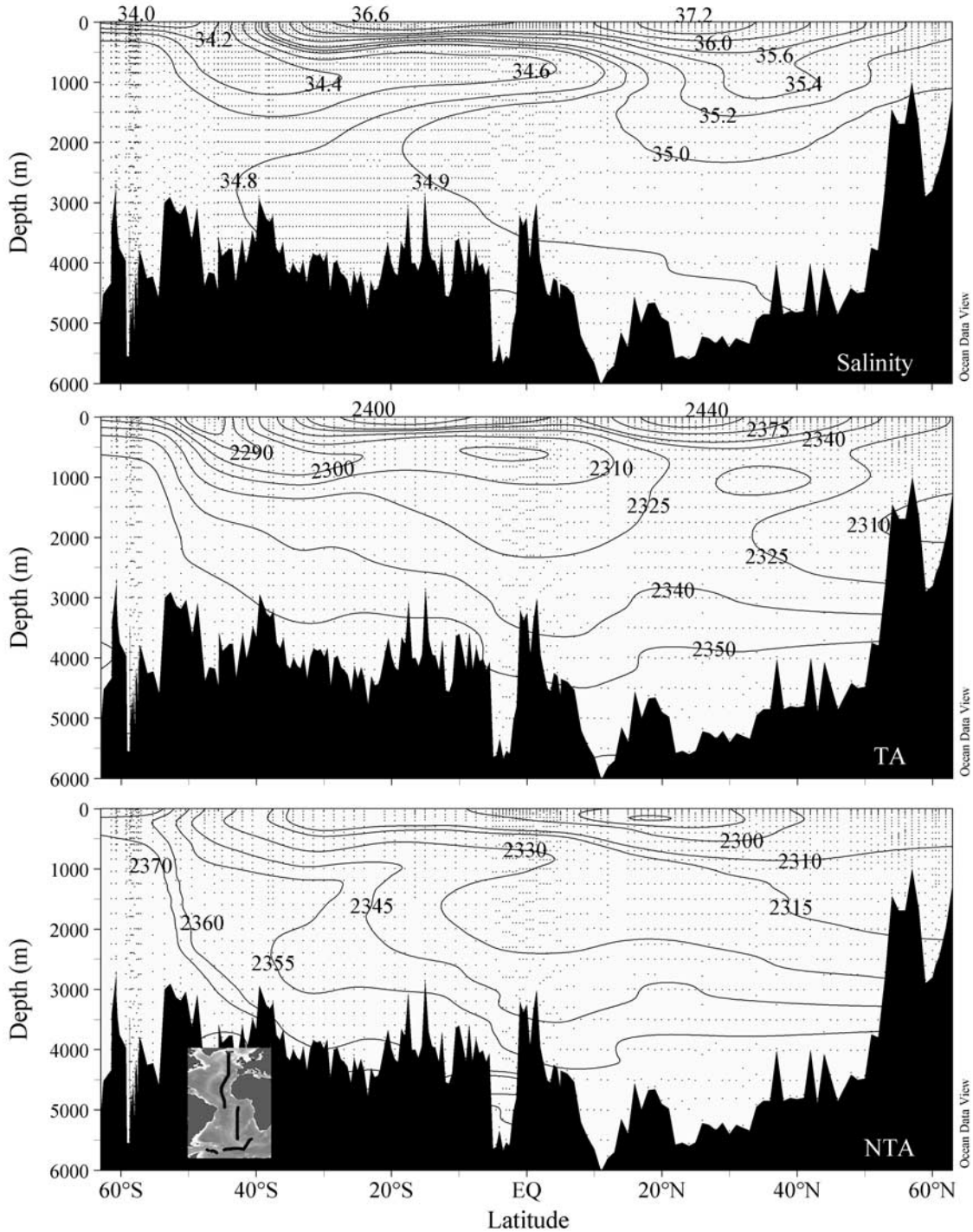

Figure 3. Meridional sections of salinity (S), total alkalinity (TA), and salinity (S = 35) normalized total alkalinity (NTA) nominally along 20°W in the eastern Atlantic Ocean. Points indicate locations of measured data. Inset shows the cruise track.

be influenced by bidirectional mixing of the assumed steady state signal of excess TA along isopycnal surfaces, while the CFC ages are determined assuming a unidirectional penetration of CFC along the same isopycnals. However, the latter effect is probably small, as it is largely accounted for by the increasing preformed TA values when moving toward the poles.

[20] Initial undersaturation of CFCs in an outcrop region will make CFC-based ages older than the true age [*Wallace et al.*, 1994; *Doney et al.*, 1997]. Because CFCs were increasing relatively rapidly in the atmosphere during the period of the study and because the dissolution rates are integrated along the path of the isopycnal over several years, a small degree of CFC disequilibrium in

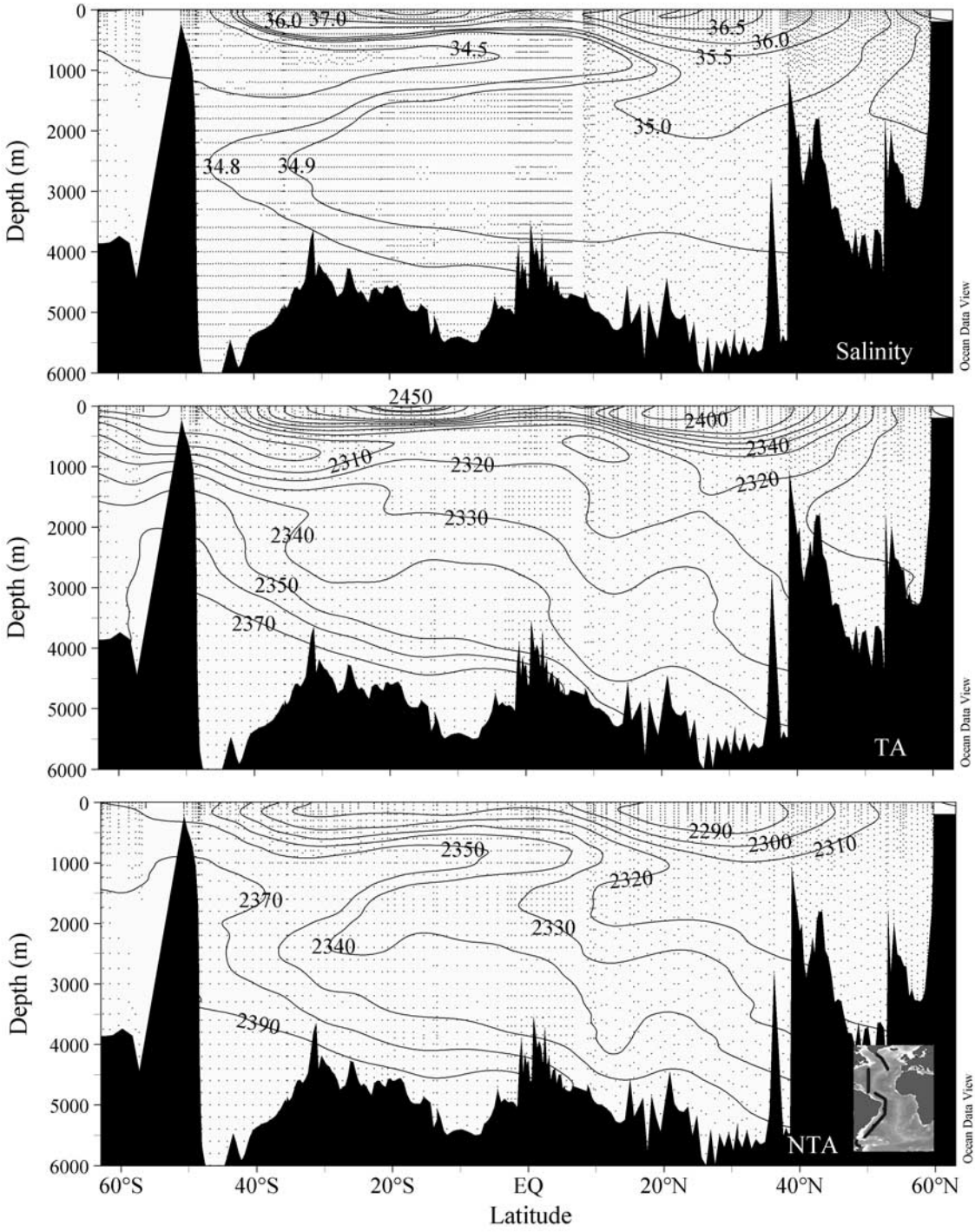

Figure 4. Meridional sections of salinity (S), total alkalinity (TA), and salinity (S = 35) normalized total alkalinity (NTA) in the western Atlantic Ocean. Points indicate locations of measured data. Inset shows the cruise track.

high-latitude waters should not significantly affect our results.

3. Results

3.1. Distribution of Alkalinity

[21] The distribution of TA in the surface mixed layer of the Atlantic Ocean is mainly controlled by the factors that govern salinity [*Broecker and Peng*, 1982; *Millero et al.*, 1998]: A variation in salinity of 1 results in a change of approximately 56 μmol kg^{-1} in TA (see equation (7)). Other nonconservative processes, such as precipitation and dissolution of biogenic $CaCO_3$, also contribute to the variability of TA, albeit to a much lesser extent [*Brewer et al.*, 1975; *Brewer and Goldman*, 1976; *Millero et al.*, 1998]. The highest concentrations of TA are

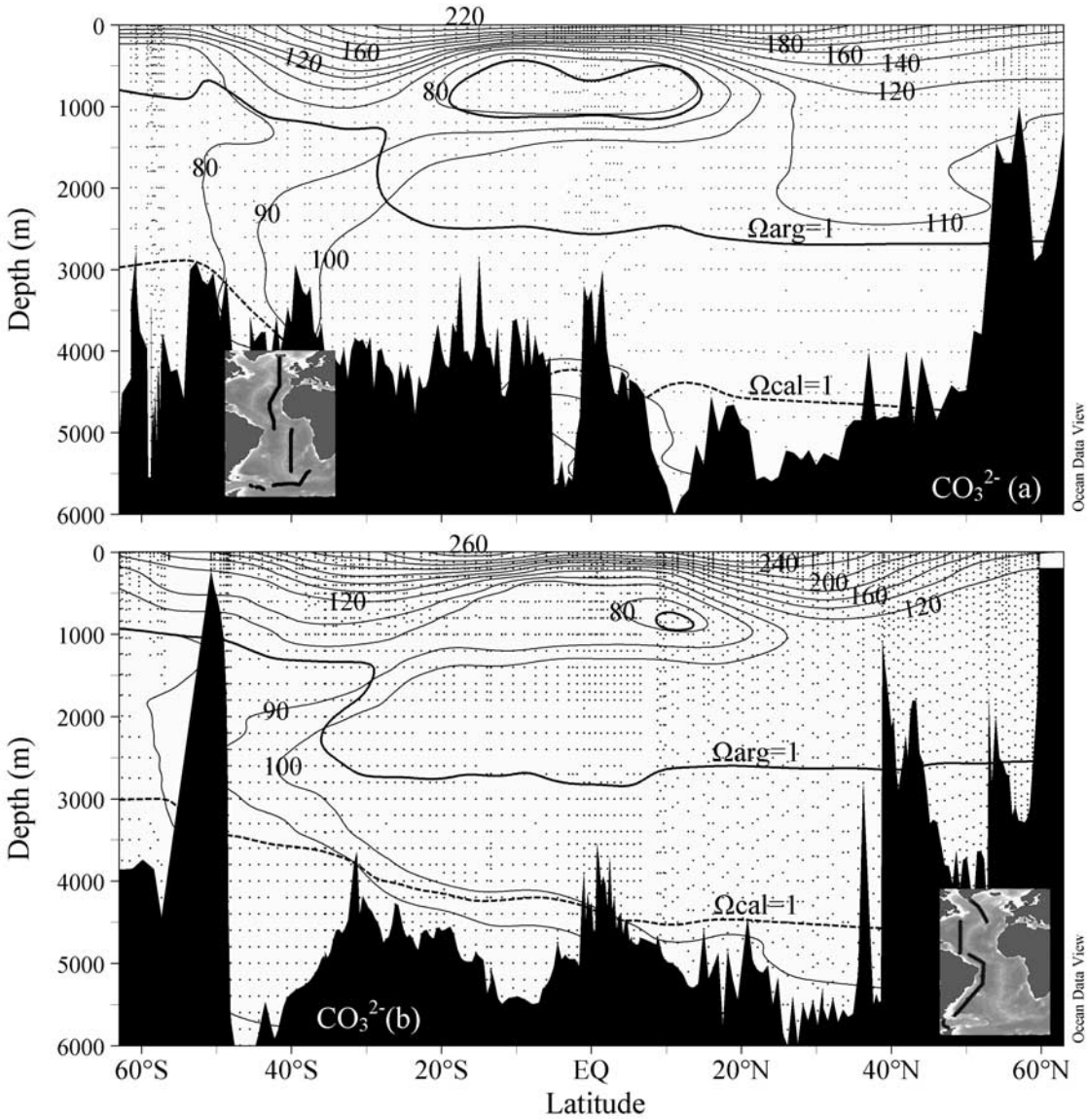

Figure 5. Meridional distributions of carbonate ion concentration [CO_3^{2-}] in the (a) eastern and (b) western Atlantic Ocean. Thick solid and dashed lines represent the aragonite (Ωarg) and calcite (Ωcal) 100% saturation horizons, respectively. Insets show the cruise tracks.

observed in the surface mixed layer waters at 30°N and 20°S where salinity maxima as high as S = 37.2 are found. From here, the salinity and TA decrease to S = 35 and TA = 2300 μmol kg^{-1} in high-latitude waters. This is in contrast with the Pacific Ocean where the highest TA values are generally found in deep waters [*Feely et al.*, 2002]. The conservative behavior of surface TA is particularly true in low-latitude regions of the Atlantic Ocean (between 40°N and 40°S). Much of the spatial and seasonal TA variability in these regions can be removed by normalizing the result to a constant salinity (S = 35) [*Lee et al.*, 1997; *Millero et al.*, 1998]. Consequently, the NTA of surface waters remains nearly constant (NTA ~ 2290 μmol kg^{-1}) from 40°S to 40°N, and increases with latitude, largely due to convective mixing of deep waters that have accumulated excess TA from $CaCO_3$ dissolution. Detailed analysis of the surface TA distribution in the Atlantic Ocean and in the other major basins are given by *Millero et al.* [1998].

[22] Figures 3 and 4 show the meridional distributions of salinity, TA, and NTA in the eastern and western Atlantic. The main features of the deep-water characteristics and circulation of the Atlantic Ocean are shown in the general structures of the TA, NTA, and salinity sections. The Antarctic Intermediate Water (AAIW) originates south of the Polar Frontal Zone and is evident as a low-salinity tongue extending to 20°N centered at about 800 m depth. The TA section also shows local minima in this region. Between the AAIW and the abyssal Antarctic Bottom Water (AABW) is the North Atlantic Deep Water (NADW), which originates in the far North Atlantic and is most evident in the salinity section. The TA section also shows a local minimum in this region, but this minimum extends southward to only 40°N due to TA

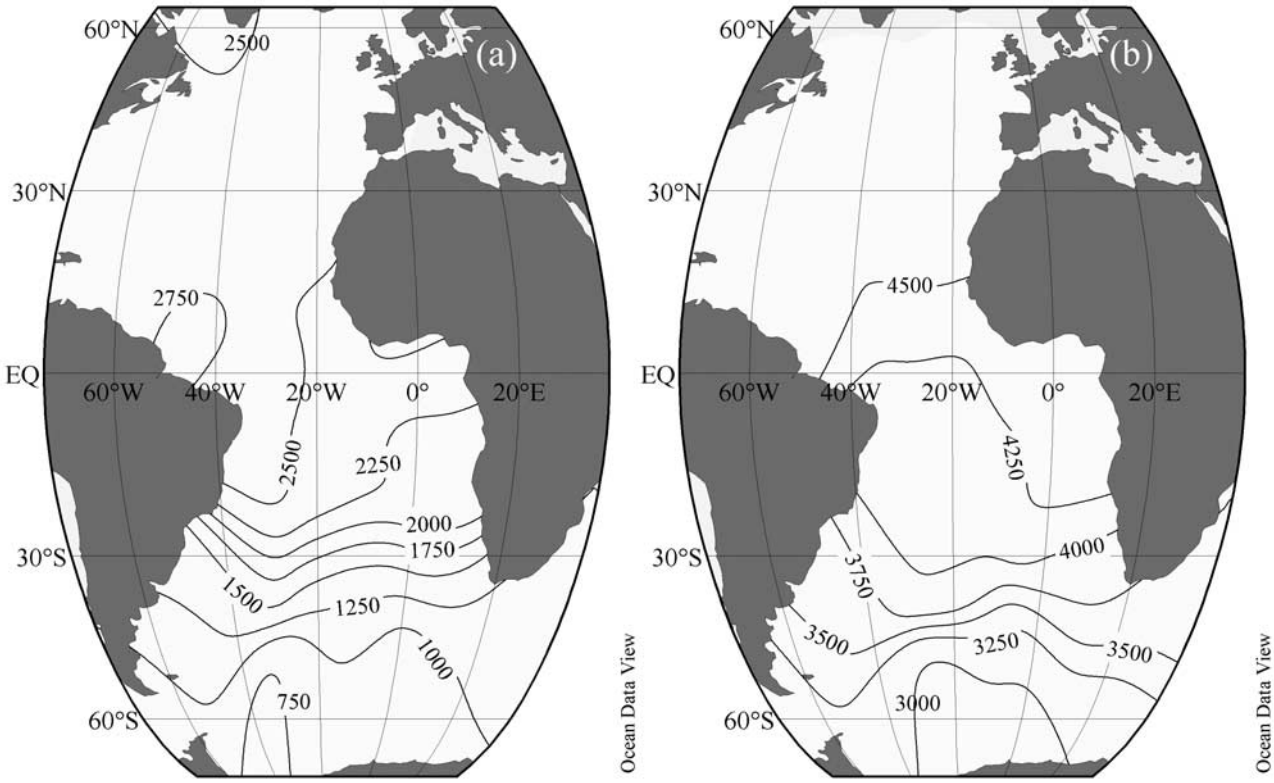

Figure 6. The 100% saturation depths (in meters) for (a) aragonite and (b) calcite calculated from water column TA and C_T concentrations. A blob of undersaturated waters with respect to aragonite centered at about 800 m between 20°S and 10°N (as shown in Figure 5a) is not shown in Figure 6a because it is a localized feature in the eastern tropical Atlantic.

increasing from $CaCO_3$ dissolution as the NADW moves to the south. The third major feature found in the intermediate water is the effect of the Mediterranean Water (MW) as a salinity maximum above the NADW. The MW maximum is clear in the eastern North Atlantic but less conspicuous in the west and in the south as it gradually loses its unique characteristics by mixing with the waters above and below it. The MW is shown as a TA maximum centered at about 1000 m depth and 35°N. Below the TA minimum layer centered at about 800 m depth in the South Atlantic, TA values gradually increase with depth. The same is true for waters deeper than 2000 m in the North Atlantic. The overall similarity between the TA and salinity sections suggests that deep-water circulation plays a critical role in the TA distribution in the deep Atlantic.

[23] The main features of the deep-water circulation of the Atlantic Ocean are not as clear in the TA sections as in the NTA and salinity sections. The NTA concentration is generally lower in waters shallower than 500 m. The lower NTA concentration in shallow warm waters is generated by a net reduction in TA resulting from the biological production of $CaCO_3$, while the higher NTA values for deep waters result from the net effect of in situ dissolution of $CaCO_3$ and oxidation of organic matter. Part of the NTA increase due to dissolution of $CaCO_3$ is offset by the release of protons from the oxidation of organic matter. This effect is generally <20% of the total NTA change in the upper Atlantic, but could be up to 40% in the deep waters of the South Atlantic. The NTA values for the NADW are lower than those for the AABW and AAIW; older water masses have more time to accumulate TA from the dissolution of $CaCO_3$.

3.2. Degree of Saturation of $CaCO_3$

[24] Previous studies have shown that the dissolution rates of $CaCO_3$ in the interior of the ocean are nonlinearly influenced by the degree of undersaturation [*Morse and Berner*, 1972; *Keir*, 1980]. It is, therefore, important to have an accurate knowledge of the saturation state of seawater with respect to aragonite and calcite. Figure 5 shows the meridional distribution of $[CO_3^{2-}]$ and the 100% saturation horizons for aragonite and calcite in the eastern and western Atlantic. The upper waters shallower than 1000 m in the South Atlantic and 2500 m in the North Atlantic are supersaturated by as much as 400% with respect to aragonite; the waters below these depths are undersaturated. The depth variations are primarily due to a difference in $[CO_3^{2-}]$ [*Morse and Berner*, 1972; *Pytkowicz*, 1973; *Broecker and Takahashi*, 1978]. An interesting feature in the eastern basin is the undersaturated water centered at 800 m between 20°S and 10°N that is sandwiched by supersaturated waters above and below. This undersaturated water is the northern extension of AAIW and may be attributed to the $[CO_3^{2-}]$ decrease caused by reaction with protons resulting from the oxida-

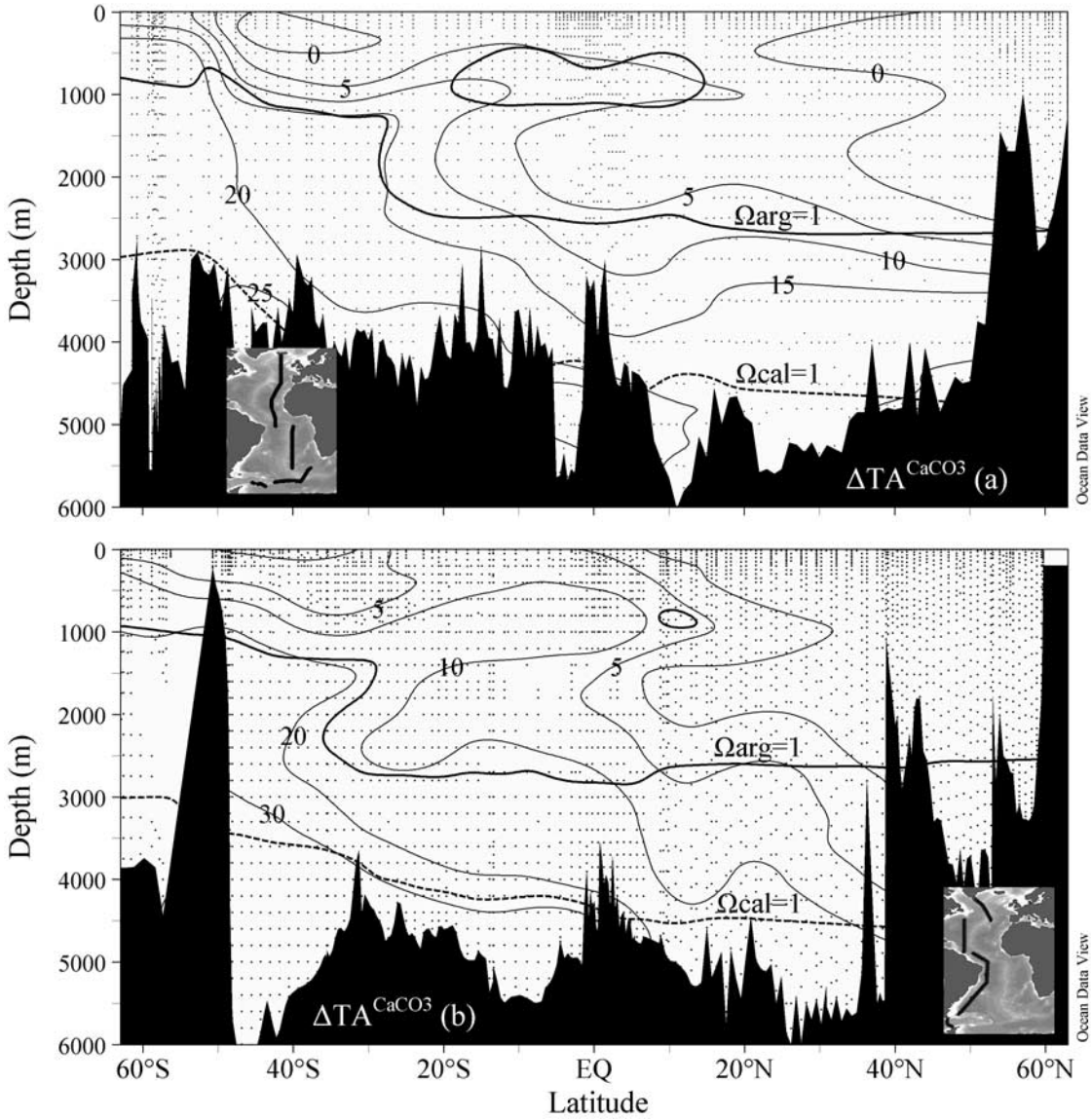

Figure 7. Meridional distribution of ΔTA^{CaCO3} in the (a) eastern and (b) western Atlantic Ocean. Thick solid and dashed lines represent the aragonite (Ωarg) and calcite (Ωcal) 100% saturation horizons, respectively. Insets show the cruise tracks.

tion of organic matter during the journey of AAIW from the surface waters of the Southern Ocean to about 1000 m in the tropical Atlantic. However, the mechanism responsible for the formation of this undersaturated water has not yet been identified.

[25] Figure 6 shows the 100% saturation depths for aragonite (Figure 6a) and calcite (Figure 6b) in the Atlantic Ocean. Both horizons are deepest in the North Atlantic and generally become shallower toward the south. The saturation depths are set by the in situ $[CO_3^{2-}]$ of waters and the pressure dependence of *K*sp-arg* and *K*sp-cal*. The degree of saturation decreases with depth because the solubility of these minerals generally increases with depth, which is attributable to several factors. First, the effect of pressure on the dissociation constants of carbonic and boric acids results in the pH decreasing and consequently in $[CO_3^{2-}]$ also decreasing. Second, remineralization of organic matter falling from the surface releases CO_2 into the water, decreasing $[CO_3^{2-}]$ and pH, and increasing the solubility of $CaCO_3$. The first effect is generally more important in deep waters, whereas the second effect is in shallow waters. Third, $CaCO_3$ becomes slightly more soluble as temperature drops with depth. However, the temperature effect is small. These combined effects cause the solubility of $CaCO_3$ to increase significantly with depth.

[26] The 100% saturation depth for aragonite is about 2500 m in areas between 20°S and 60°N, and decreases to about 1000 m in areas south of 30°S. The saturation depths for aragonite are generally deeper in the western basin than in the eastern basin (Figure 6) because the older waters in the eastern basin have lower $[CO_3^{2-}]$ due to accumulation of protons from the oxidation of organic matter. The 100% saturation depth for calcite is signifi-

cantly deeper than that for aragonite. It is slightly deeper than 4000 m in the North Atlantic and decreases to 3000−4000 m in the South Atlantic. About 58% of the water in the Atlantic Ocean is supersaturated with respect to aragonite, while 80−90% of the water is supersaturated with respect to calcite. Overall, the waters in the Atlantic Ocean are much less corrosive to $CaCO_3$ particles than those in the other major basins.

3.3. In Situ Dissolution Rates of $CaCO_3$

[27] The dissolution rates presented in this paper were separately determined for three different regions (70°N −40°N, 40°N−40°S, and 40°S−70°S). For each region the rates were also separately estimated for the upper waters (<1500 m) and intermediate and deep waters (>1500 m).

[28] The meridional distribution of ΔTA^{CaCO3} in the Atlantic Ocean is shown in Figure 7. The major circulation features of the Atlantic Ocean are evident in the structures of the ΔTA^{CaCO3} section. However, the general increase in the ΔTA^{CaCO3} concentration with depth suggests that the alkalinity signal in deep waters is produced mainly by in situ dissolution of $CaCO_3$ particles. The ΔTA^{CaCO3} concentration ranges from <10 μmol kg^{-1} in the upper ocean to 20−30 μmol kg^{-1} in deep waters. The discernable ΔTA^{CaCO3} increase (>10 μmol kg^{-1}) begins at about 800 m in the South Atlantic but at about 2500 m in the North Atlantic (north of 40°N). The depth at which the significant ΔTA^{CaCO3} increase occurs is approximately consistent with the aragonite 100% saturation horizon. Below this depth, the values of ΔTA^{CaCO3} increase rapidly over several hundred meters and then increase gradually from there to the bottom of the ocean. Much of the ΔTA^{CaCO3} increase occurs in waters between the aragonite and calcite 100% saturation horizons, suggesting that the degree of saturation of seawaters is a primary factor controlling the extent of in situ dissolution of $CaCO_3$.

[29] Dissolution rates for waters shallower than 1500 m in Figure 8a were estimated using CFC-11 apparent ages. Rates for the intermediate North Atlantic waters between σ_4 = 45.4 and σ_4 = 45.8 in Figure 8b were also estimated using CFC-11 ages, while rates for the deep North Atlantic (σ_4 > 45.8) and South Atlantic waters were obtained using Δ^{14}C-derived ages. This analysis helps us identify where and to what extent $CaCO_3$ dissolution occurs in the water column.

[30] Rates in the South Atlantic (south of 40°S) are nearly zero in waters less than σ_θ = 27.4 and increase to a maximum rate of ~0.28 μmol kg yr^{-1} at σ_θ = 27.6. Rates in the North Atlantic (north of 40°N) are not statistically significant at σ_θ < 27.8 because values of ΔTA^{CaCO3} are typically less than 10 μmol kg^{-1}, which is within the uncertainty in estimating ΔTA^{CaCO3}. Maximum dissolution rates in the North Atlantic occur in waters near the mean aragonite saturation horizon of approximately 2500 m (Figure 8b). The reduction in depth where the maximum rate occurs is consistent with the corresponding change in the aragonite 100% saturation horizon. Below σ_θ = 27.8 in the South Atlantic the dissolution rates sharply decrease to <0.1 μmol kg yr^{-1}, whereas the rates in the North Atlantic increase (Figure 8b).

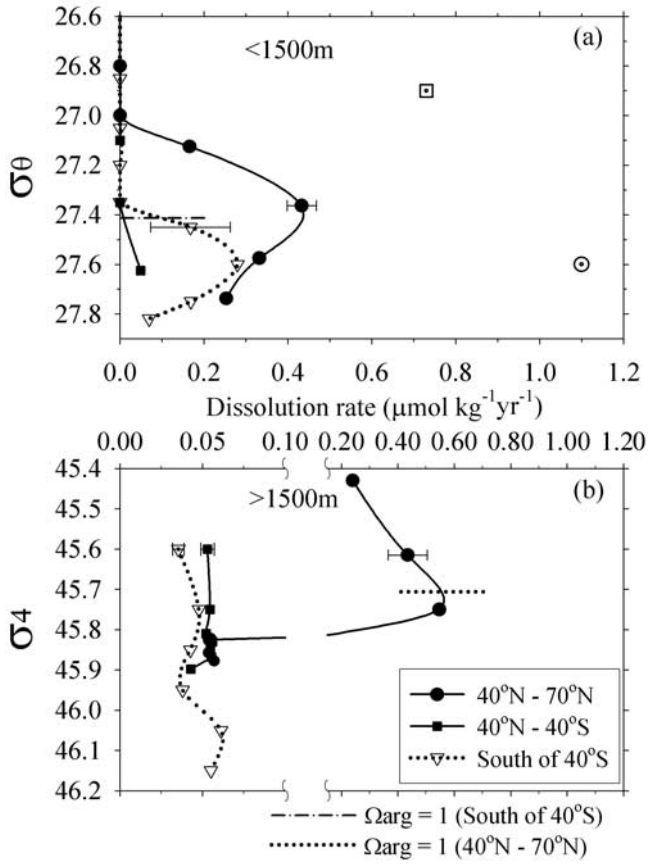

Figure 8. Plots of estimated $CaCO_3$ dissolution rates as a function of (a) σ_θ (potential density referenced to the surface) for waters shallower than 1500 m and (b) σ_4 (potential density referenced to 4000 dbar) for waters deeper than 1500 m. All dissolution rates in Figure 8a were estimated using CFC-11 apparent ages. Rates for the intermediate North Atlantic waters between σ_4 = 45.4 and σ_4 = 45.7 in Figure 8b were also estimated using CFC-11 apparent ages, while other rates for the deep North Atlantic and South Atlantic waters in Figure 8b were obtained using Δ^{14}C-derived ages. Highest rates in the north Indian Ocean (dot in a square) and the South Pacific Ocean (dot in a circle) are shown for comparison (taken from *Sabine et al.* [2002a] and *Feely et al.* [2002]). Error bars for our results are standard deviations from mean rates for all the isopycnal surfaces of each region.

The rates at greatest densities of the upper waters (σ_θ ~ 27.8) in the South Atlantic are close to the deep-water values that are estimated using the Δ^{14}C method, suggesting no bias between the two methods of determining dissolution rates. The dissolution in low latitudes (between 40°S and 40°N) occurs in waters with densities greater than σ_θ = 27.4, but observed rates are lower than 0.05 μmol kg yr^{-1} and significantly lower than the rates at higher latitudes.

[31] Dissolution rates in the intermediate and deep waters of the South Atlantic (>1500 dbar) are in the range of 0.030−0.061 μmol kg^{-1} yr^{-1} (Figure 8b). These rates

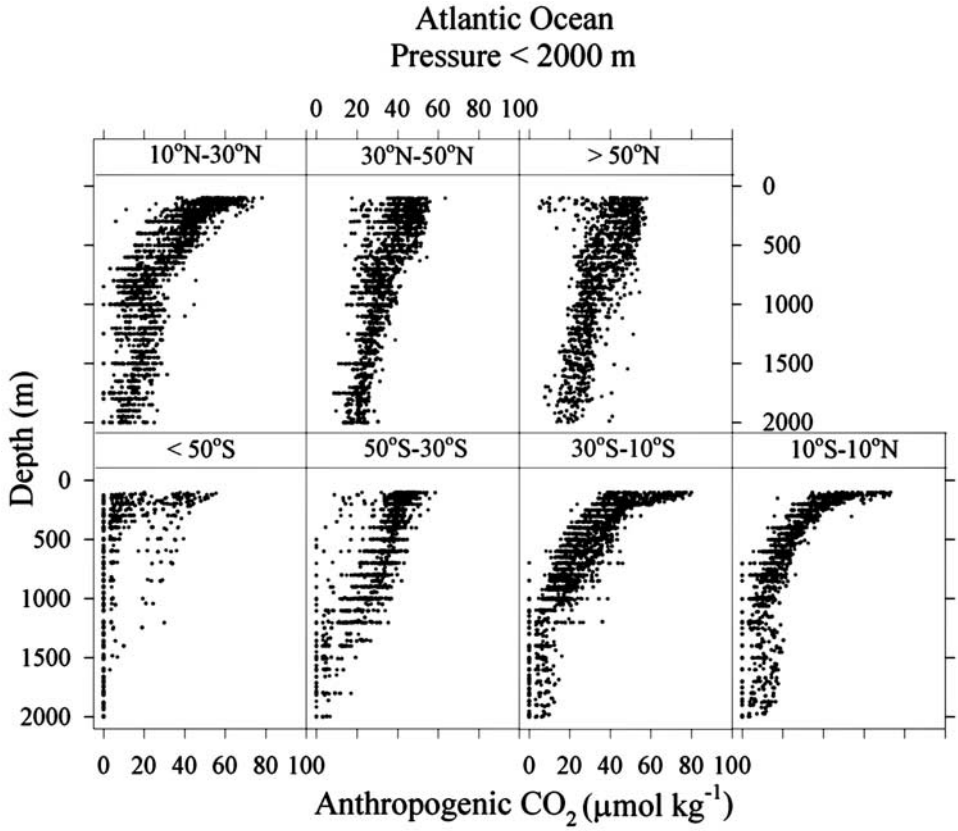

Figure 9. Profiles of anthropogenic CO_2 concentration in 20° latitude belts between 70°S and 70°N. Data collected in waters shallower than 2000 m are plotted.

are up to an order of magnitude lower than those found in shallower waters. In contrast, the rates in the North Atlantic for densities σ_4 (referenced to 4000 dbar) between 45.4 and 45.8 are in the range of 0.24−0.54 μmol kg^{-1} yr^{-1} and then sharply decrease to <0.1 μmol kg yr^{-1} at σ_4 = 45.83. The dissolution rates south of 40°S are lower than the values in the rest of the Atlantic Ocean at densities σ_4 between 45.6 and 45.9, but then increase to a maximum of 0.061 at σ_4 = 46.05.

4. Discussion

4.1. Upward Migration of the Aragonite 100% Saturation Horizon

[32] The protons ($[H^+]$) formed by dissolution of anthropogenic CO_2 in seawater lower the pH so that some of them combine with $[CO_3^{2-}]$ to form $[HCO_3^-]$. Thus addition of anthropogenic CO_2 into the ocean decreases $[CO_3^{2-}]$, which in turn lowers saturation states of seawater with respect to aragonite or calcite. Figure 9 shows profiles of anthropogenic CO_2 concentration in 20° latitude belts between 70°S and 70°N (Lee et al., submitted manuscript, 2003). The surface concentrations of anthropogenic CO_2 (typically 40−60 μmol kg^{-1}) are highest in the subtropical waters and decrease toward higher latitudes (20−40 μmol kg^{-1}). Anthropogenic CO_2 generally penetrates to shallower depths in the tropical and subtropical regions, and to deeper water as latitude increases. However, the symmetrical feature of vertical penetration of anthropogenic CO_2 between the two hemispheres breaks down toward the poles: Anthropogenic CO_2 penetrates all the way down to the bottom in the northern high-latitude regions, whereas in sharp contrast to this the shallowest penetrations are observed in the high-latitude Southern Ocean. The distribution of anthropogenic CO_2 in the Atlantic Ocean shows that a significant part of the Atlantic Ocean has been affected by the vertical penetration of anthropogenic CO_2.

[33] In regions between 30°N and 30°S in the Atlantic Ocean the aragonite 100% saturation horizon for the preindustrial era is nearly the same as that for the present day (Figure 10, solid and dashed lines, respectively). By contrast, the aragonite 100% saturation horizon has migrated upward by approximately 100−150 m in the South Atlantic and in the western North Atlantic. The penetration of anthropogenic CO_2 in the eastern North Atlantic is not sufficiently deep to affect the saturation horizon. The calcite 100% saturation depths in the Atlantic Ocean are typically deeper than 4000 m and are not affected by the penetration of anthropogenic CO_2; therefore they are not shown in Figure 10. Waters contaminated by anthropogenic CO_2 have experienced changes in saturation states with respect to aragonite. Upward migration of the aragonite saturation horizon in the Atlantic Ocean during the industrial era suggests that $CaCO_3$ particles falling from the surface may begin to

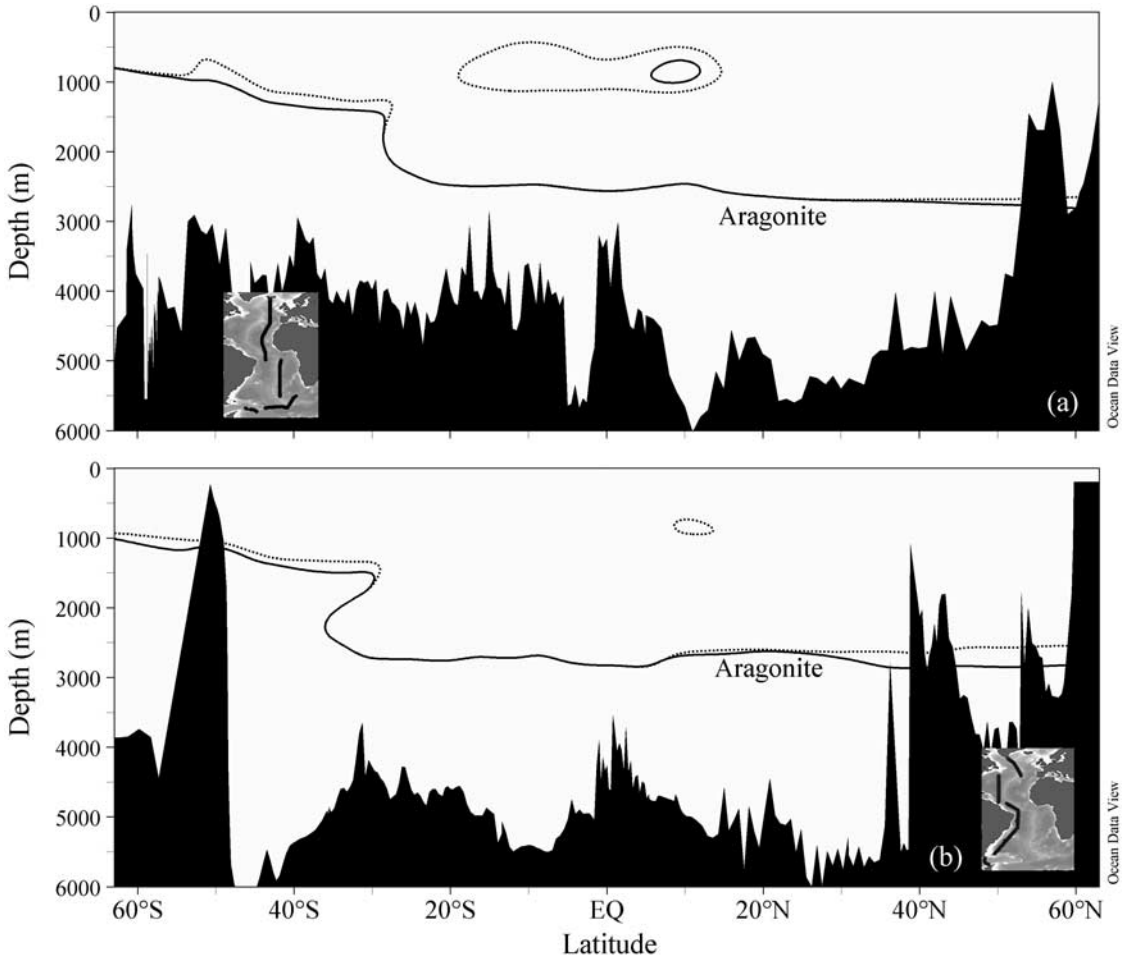

Figure 10. Comparison of the aragonite 100% saturation horizons for the present day and for the preindustrial era in the (a) eastern and (b) western Atlantic Ocean. Thick solid and dashed lines represent the aragonite saturation horizons for the preindustrial era and the present day, respectively. Insets show the cruise tracks.

dissolve at shallower depths, modifying the in situ dissolution of $CaCO_3$ and the supply of $CaCO_3$ to the sediments.

4.2. Possible Mechanisms Responsible for In Situ Dissolution of $CaCO_3$

[34] Many of the currently available in situ dissolution rates of $CaCO_3$ particles have been measured at different saturation states (or depths) by determining the decrease in mass of $CaCO_3$ particles [*Byrne et al.*, 1984]. Our dissolution-rate estimate differs from previous estimates in that the estimate not only depends on the decrease in the mass of sinking $CaCO_3$ particles but also on the total mass flux. That is, for a similar decrease in the mass of sinking $CaCO_3$ particles, a greater dissolution rate of $CaCO_3$ will be inferred for areas with greater $CaCO_3$ production in the overlying water column.

[35] The spatial variability of the dissolution rate shown in Figure 8 could be attributed partly to regional variability in the rain rate of $CaCO_3$ [see *Lee*, 2001, Figure 4]. The net $CaCO_3$ production estimated by integrating seasonal decreases in *P*TA in the mixed layer is virtually zero in subtropical areas between 40°and 40°S [*Lee*, 2001], as *P*TA is constant throughout the year [*Bates et al.*, 1996; *Millero et al.*, 1998]. The estimated net $CaCO_3$ production in the North Atlantic (>40°) is much higher than in the South Atlantic, which is consistent with the contention that ballasting of organic matter by $CaCO_3$ is more important in the North Atlantic than in the rest of the world [*Berger*, 1992; *Armstrong et al.*, 2002]. The higher dissolution rates in the North Atlantic are attributable to higher $CaCO_3$ rain rates. Insignificant dissolution rates in the subtropical Atlantic are consistent with insignificant rain rates. In waters with the same degree of saturation with aragonite or calcite, the amount of $CaCO_3$ exported from the surface will determine the extent of the in situ $CaCO_3$ dissolution.

[36] The significant increase in ΔTA^{CaCO3} along isopycnal surfaces begins at 2500 m in the North Atlantic and 800 m in the South Atlantic, at or below the aragonite 100% saturation horizon. This ΔTA^{CaCO3} increase implies discernable rates of $CaCO_3$ dissolution, suggesting that a significant portion of $CaCO_3$ production in the North Atlantic is dissolved in the water column. However, we

Table 2. Estimated Water Column Inventory of ΔTA^{CaCO3} in the Atlantic Ocean[a]

Latitude Belt	Area, (10^{12} m^2)	Volume, 10^{16} m^3	$CaCO_3$ Production Rate, mol C yr^{-1} [*Lee*, 2001]	$CaCO_3$ Dissolution Rate, mol C yr^{-1}
70°N–40°N	12.4	2.6	12.5×10^{12}	$3.6 \pm 0.5 \times 10^{12}$[b]
40°–40°S	49.1	19.7	15.0×10^{12}	$7.7 \pm 0.7 \times 10^{12}$
40°S–70°S	18.5	7.1	8.3×10^{12}	$5.4 \pm 2.1 \times 10^{12}$
Total			35.8×10^{12}	$16.7 \pm 3.3 \times 10^{12}$

[a]We equate this to the inventory of in situ dissolution of $CaCO_3$.
[b]The $CaCO_3$ dissolution rate for 70°N–40°S does not include integrated rates shallower than 1500 m, because values of ΔTA^{CaCO3} for these waters are <10 μmol kg^{-1}, which is close to the uncertainty in estimating ΔTA^{CaCO3}.

cannot rule out that other mechanisms contribute to the excess ΔTA^{CaCO3} near the aragonite saturation horizon. One mechanism is dissolution of $CaCO_3$ in the guts of zooplankton and in fecal pellets. This mechanism was originally proposed by *Takahashi* [1975] and later by others [*Bishop et al.*, 1980; *Pond et al.*, 1995; *Milliman et al.*, 1999; *Jansen and Wolf-Gladrow*, 2001]. Several laboratory experiments, however, have shown that the pH in guts of grazers ranges from neutral to alkaline, which is an unfavorable condition for dissolution of $CaCO_3$ [*Harris*, 1994; *Pond et al.*, 1995]. Dissolution therefore may occur during the early feeding stages [*Pond et al.*, 1995]. The other proposed mechanisms include increased dissolution of $CaCO_3$ in microenvironments where microbial oxidation of organic matter occurs [*Jansen and Wolf-Gladrow*, 2001] and dissolution of the more soluble phases of $CaCO_3$ such as pteropods and high-magnesium calcite [*Betzer et al.*, 1984; *Byrne et al.*, 1984; *Morse and Mackenzie*, 1990; *Sabine et al.*, 1995]. An additional mechanism recently proposed by *Chen* [2002] is that TA generated from the decomposition of organic matter occurring in shelf sediments could be a significant source of excess TA for subsurface waters in the open ocean. In oxygen-depleted shelf sediments, manganese, iron, and sulfate are used as electron accepters to decompose organic matter, all of which increase TA. It is, however, not possible to quantify the effect of shelf waters high in NTA because the horizontal extent of the shelf waters is not known very well. More than one mechanism may collectively contribute to the positive ΔTA^{CaCO3} in supersaturated waters with respect to calcite, although one of them may dominate in certain environments [*Milliman et al.*, 1999].

4.3. $CaCO_3$ Budget in the Atlantic Ocean

[37] To construct the basin-scale $CaCO_3$ budget we need to know the net $CaCO_3$ production in the euphotic zone and what fraction of it dissolves within the water column before reaching the seafloor for burial. To quantify the amount of $CaCO_3$ dissolved in the water column, the ΔTA^{CaCO3} must be corrected for TA input from the dissolution of sedimentary $CaCO_3$. Existing estimates of global net $CaCO_3$ production are based on direct measurements (e.g., calcification rates and sediment-trap fluxes) or models that combine information about ocean circulation with *P*TA variations. Estimates range from 42×10^{12} mol C yr^{-1} to 170×10^{12} mol C yr^{-1} [see *Milliman et al.*, 1999; *Sarmiento et al.*, 2002]. Recently, *Lee* [2001] estimated a global net $CaCO_3$ production of $[92 \pm 25] \times 10^{12}$ mol C yr^{-1} by integrating seasonal decreases in *P*TA in the mixed layer. This value is approximately three times higher than a recently revised trap-based estimate of 34×10^{12} mol C yr^{-1} at 2000 m depths [*Iglesias-Rodriguez et al.*, 2002]. In our calculation of the $CaCO_3$ budget we used the value of $[35.8 \pm 9.5] \times 10^{12}$ mol C yr^{-1} obtained by *Lee* [2001] for the Atlantic Ocean.

[38] The total amount of $CaCO_3$ dissolved in the Atlantic Ocean was estimated by integrating dissolution rates for all the isopycnal surfaces. The inventory of the total ΔTA^{CaCO3} (*TOTAL*-ΔTA^{CaCO3}) for each of three latitude belts (70°N–40°N, 40°N–40°S, and 40°S–70°S) was determined by integrating the mean profile (*f-mean*) of dissolution rates from surface (*SFC*) to a mean bottom depth (*MD*) (Table 2),

$$TOTAL\text{-}\Delta TA^{CaCO3}(lat.\,1, lat.\,2) = \int A(lat.\,1, lat.\,2) \times f\text{-}mean\ \mathrm{dz}. \quad (8)$$

[39] Since our rates were estimated on isopycnal surfaces, a mean depth-density relationship was derived for each of the three latitude blocks (see Figure 8) and applied to the respective density-dissolution-rate profile, to derive a mean depth-dissolution-rate profile for each latitude block. This method yields a basin-scale dissolution rate of $[16.7 \pm 3.3] \times 10^{12}$ mol C yr^{-1}, which is probably an overestimate because part of the excess ΔTA^{CaCO3} may be derived from sulfate reduction [*Chen*, 2002] and dissolution of $CaCO_3$ occurring in sediments.

[40] Biogeochemical processes within the sediment alter the sedimentation and burial of $CaCO_3$ particles once they reach the seafloor. A major benthic process influencing $CaCO_3$ preservation and dissolution in deep-sea sediments is the oxidation of organic matter [*Emerson and Bender*, 1981]. Several previous studies have confirmed that $CaCO_3$ dissolves in response to metabolic CO_2 produced during degradation of organic matter. Different techniques yield $CaCO_3$ dissolution rates in sediments with mixed results: In situ microelectrode profiles have shown the occurrence of $CaCO_3$ dissolution above the calcite saturation horizon [*Archer et al.*, 1989; *Martin and Sayles*, 1996; *Hales and Emerson*, 1997], whereas benthic-chamber incubation experiments suggest that the metabolic CO_2-driven dissolution is not as important as suggested by microelectrode measurements [*Jahnke*, 1994; *Jahnke et al.*, 1994]. The ΔTA^{CaCO3} contribution from the dissolution of sedimentary $CaCO_3$ was estimated here from a limited number of in situ measurements. The entire Atlantic basin was given a mean $CaCO_3$ dissolution rate of 7 ± 4 μmol cm^{-2} yr^{-1}, as obtained from in situ electrode mea-

surements in sediments of the Ceara Rise (5°N, 45°) of the western tropical Atlantic [*Martin and Sayles*, 1996; *Hales and Emerson*, 1997]. This method yields a rate of sedimentary $CaCO_3$ dissolution of $[5.6 \pm 3.2] \times 10^{12}$mol C yr^{-1}, accounting for 34% of the in situ dissolution rate of $[16.7 \pm 3.3] \times 10^{12}$ mol C yr^{-1} for the entire Atlantic basin.

[41] The resulting water column dissolution rate for the entire Atlantic corrected for the sedimentary dissolution of $CaCO_3$ is 11.1×10^{12} mol C yr^{-1}, which equates to a significant fraction (31%) of the total net $CaCO_3$ production of $[35.8 \pm 9.5] \times 10^{12}$ mol C $yr-^{1}$ for the same area. Our budget calculation would also imply a $CaCO_3$ accumulation rate of 25.6×10^{12} mol C yr^{-1} for the Atlantic, which is significantly greater than the accumulation rate of 5.4×10^{12} mol C yr^{-1} for the same area determined by *Milliman and Droxler* [1996] and *Catubig et al.* [1998] based on the measured $CaCO_3$ content in numerous deep-sea sediment samples. The estimate of 5.4×10^{12} mol C yr^{-1} is close to 50% of the global deep-sea $CaCO_3$ accumulation rate. Although the discrepancy between these two independent estimates of the $CaCO_3$ accumulation rate appears large, the difference may be insignificant considering that estimations of the production and water column dissolution of $CaCO_3$, and sedimentary inputs of $CaCO_3$ have potential uncertainties of at least 100% [see *Iglesias-Rodriguez et al.*, 2002, Table 1], which are considerably greater than those used in our budget calculation. Therefore the closure of the $CaCO_3$ budget is presently far from complete and requires a global synthesis of data on alkalinity and sediment trapping. This will also require time series measurements of $CaCO_3$ production along with satellite and ground-based data.

5. Conclusion

[42] The ΔTA^{CaCO3} values calculated using WOCE/JGOFS/OACES Atlantic CO_2 survey data suggest that significant $CaCO_3$ dissolution occurs in undersaturated waters of 2500−3000 m depth in the North Atlantic and of 500−1000 m depth in the South Atlantic. The excess ΔTA^{CaCO3} rapidly increases at the aragonite 100% saturation horizon. Our analysis suggests that the excess ΔTA^{CaCO3} in intermediate waters results from water column dissolution of $CaCO_3$ particles. Our results generally support the conclusion, drawn from particle-flux data obtained during the North Atlantic Bloom Experiment, that a significant fraction (30−40%) of the total $CaCO_3$ flux dissolves in the water column at 1000−4000 m depth [*Yu et al.*, 2001]. Our results are also consistent with the suggestion by *Byrne et al.* [1984], *Betzer et al.* [1984], and *Milliman et al.* [1999] that more soluble forms of $CaCO_3$ such as aragonite and high-magnesium calcite are a source of excess ΔTA^{CaCO3} in the upper water column. This shallow-water dissolution of $CaCO_3$ creates excess TA in the upper ocean, which is important in the short-term buffering of fossil-fuel CO_2 taken up by the ocean.

[43] **Acknowledgments.** This work would not have been possible without the effort of many scientists particularly responsible for the carbon and CFC measurements on the ships during the WOCE/JGOFS/OACES global CO_2 survey conducted between 1990 and 1998. We wish to thank all of the U.S. and European scientists who contributed to the Atlantic data set that was compiled for the Global Ocean Data Analysis Project (GLODAP), and Andrew Dickson and an anonymous reviewer for constructive suggestions on the manuscript. This work was partially supported by grant R01-2002-000-00549-0 (2002) from the Basic Research Program of the Korea Science and Engineering Foundation (K. L.), by the Brain Korea 21 Project in 2003 (K. L.), by the National Oceanic and Atmospheric Administration Office of Oceanic and Atmospheric Research (C. S., R. A. F., R. W., J. L. B., and F. J. M.; contract GC 90−220), by the National Science Foundation (C. S.; contract OCE-0137144, R. M. K., and F. J. M.), by the Joint Institute for the Study of the Atmosphere and Ocean, and by the Cooperative Institute of Marine and Atmospheric Studies(K. L.).

References

Anderson, L. A., and J. L. Sarmiento, Redfield ratios of remineralization determined by nutrient data analysis, *Global Biogeochem. Cycles*, *8*, 65–80, 1994.

Archer, D., S. Emerson, and C. R. Smith, Dissolution of calcite in deep-sea sediments: pH and O_2 microelectrode results, *Geochim. Cosmochim. Acta*, *53*, 2831–2845, 1989.

Armstrong, R. A., C. Lee, J. I. Hedges, S. Honjo, and S. G. Wakeham, A new mechanistic model for organic carbon fluxes in the ocean based on the quantitative association of POC with ballast minerals, *Deep Sea Res., Part II*, *49*, 219–236, 2002.

Bates, N. R., A. F. Michaels, and A. H. Knap, Seasonal and interannual variability of oceanic carbon dioxide species at the U.S. JGOFS Bermuda Atlantic time-series study (BATS) site, *Deep Sea Res., Part II*, *43*, 347–384, 1996.

Berger, W. H., Global map of ocean productivity, in *Productivity of the Ocean: Present and Past*, edited by V. S. Smetacek and G. Wefer, pp. 429–455, John Wiley, Hoboken, N. J., 1992.

Betzer, P. R., R. M. Byrne, J. G. Acker, C. S. Lewis, R. R. Jolly, and R. A. Feely, The oceanic carbonate system: A reassessment of biogenic controls, *Science*, *226*, 1074–1077, 1984.

Bishop, J. K. B., R. W. Collier, D. R. Kettens, and J. M. Edmond, The chemistry, biology and vertical flux of particulate matter from the upper 1500 m of the Panama Basin, *Deep Sea Res., Part I*, *27*, 615–640, 1980.

Brewer, P. G., and J. Goldman, Alkalinity changes generated by phytoplankton growth, *Limnol. Oceanogr.*, *21*, 108–117, 1976.

Brewer, P. G., G. T. F. Wong, M. P. Bacon, and D. W. Spencer, An oceanic calcium problem?, *Earth Planet. Sci. Lett.*, *26*, 81–87, 1975.

Broecker, W. S., 'NO', a conservative water-mass tracer, *Earth Planet. Sci. Lett.*, *23*, 100–107, 1974.

Broecker, W. S., and T.-H., Peng, *Tracers in the Sea*, 690 pp., Eldigeo Press, Palisades, N. Y., 1982.

Broecker, W. S., and T. Takahashi, The relationship between lysocline depth and in situ carbonate ion concentration, *Deep Sea Res., Part I*, *25*, 65–95, 1978.

Byrne, R. H., J. G. Acker, P. R. Betzer, R. A. Feely, and M. H. Cates, Water column dissolution of aragonite in the Pacific Ocean, *Nature*, *312*, 321–326, 1984.

Catubig, N. R., D. E. Archer, R. Francois, P. de Penocal, W. Howard, and E. F. Yu, Global deep-sea burial rate of calcium carbonate during the last glacial maximum, *Paleoceanography*, *13*, 298–310, 1998.

Chen, C.-T. A., Decomposition of calcium carbonate and organic carbon in the deep oceans, *Science*, *201*, 735–736, 1978.

Chen, C.-T. A., Shelf-vs. dissolution-generated alkalinity above the chemical lysocline, *Deep Sea Res., Part II*, *49*, 5365–5375, 2002.

Dickson, A. G., An exact definition of total alkalinity and a procedure for the estimation of alkalinity and total inorganic carbon from titration data, *Deep Sea Res., Part I*, *28*, 609–623, 1981.

Dickson, A. G., and F. J. Millero, A comparison of the equilibrium constants for the dissociation of carbonic acid in seawater media, *Deep Sea Res., Part I*, *34*, 1733–1743, 1987.

Doney, S. C., and J. L. Bullister, A chlorofluorocarbon section in the eastern North Atlantic, *Deep Sea Res., Part I*, *39*, 1857–1883, 1992.

Doney, S. C., W. J. Jenkins, and J. L. Bullister, A comparison of ocean tracer dating techniques on a meridional section in the eastern North Atlantic, *Deep Sea Res., Part I*, *44*, 603–626, 1997.

Emerson, S. R., and M. Bender, Carbon fluxes at the sediment-water interface of the deep-sea: Calcium carbonate preservation, *J. Mar. Res.*, *39*, 139–162, 1981.

Feely, R. A., et al., In situ calcium carbonate dissolution in the Pacific Ocean, *Global Biogeochem. Cycles*, *16*(4), 1144, doi:10.1029/2002GB001866, 2002.

François, R., S. Honjo, R. Krishfield, and S. Manganini, Running the gauntlet in the twilight zone: The effects of midwater processes on the biological pump, *U.S. JGOFS News*, *11*(4), 4–6, 2002.

Godwin, H., Half-life of radiocarbon, *Nature*, *195*, 984, 1962.

Gruber, N., and J. L. Sarmiento, Global patterns of marine nitrogen fixation and denitrification, *Global Biogeochem. Cycles*, *11*, 235–266, 1997.

Gruber, N., J. L. Sarmiento, and T. F. Stocker, An Improved method for detecting anthropogenic CO_2 in the oceans, *Global Biogeochem. Cycles*, *10*, 809–837, 1996.

Hales, B., and S. Emerson, Calcite dissolution in sediments of the Ceara Rise: In situ measurements of porewater O_2, pH, and CO_2(aq), *Geochim. Cosmochim. Acta*, *61*, 501–514, 1997.

Harris, R. P., Zooplankton grazing on the coccolithophore Emiliani huxleyi and its role in the inorganic carbon flux, *Mar. Biol.*, *119*, 431–439, 1994.

Iglesias-Rodriguez, D., R. Armstrong, R. A. Feely, R. Hood, J. Kleypas, J. D. Milliman, C. L. Sabine, and J. Sarmiento, Progress made in study of ocean's calcium carbonate budget, *Eos Trans. AGU*, *83*(34), 365, 2002.

Ingle, S. E., Solubility of calcite in the ocean, *Mar. Chem.*, *44*, 205–220, 1975.

Jahnke, R. A., Calcium carbonate dissolution at the seafloor: Direct observations with in situ benthic flux chamber, *Eos Trans. AGU*, *75*, 363, 1994.

Jahnke, R. A., D. B. Craven, and J.-F. Gaillard, The influence of organic matter diagenesis on $CaCO_3$ dissolution at the deep-sea floor, *Geochim. Cosmochim. Acta*, *58*, 2799–2809, 1994.

Jansen, H., and D. A. Wolf-Gladrow, Carbonate dissolution in copepod guts: A numerical model, *Mar. Ecol. Prog. Ser.*, *221*, 199–207, 2001.

Johnson, K. M., K. D. Wills, D. B. Butler, W. K. Johnson, and C. S. Wong, Coulometric total carbon dioxide analysis for marine studies: Maximizing the performance of an automated continuous gas extraction system and coulometric detector, *Mar. Chem.*, *44*, 167–187, 1993.

Kanamori, S., and H. Ikegami, Calcium-alkalinity relationship in the North Pacific, *J. Oceanogr. Soc. Jpn.*, *38*, 57–62, 1982.

Keir, R. S., The dissolution kinetics of biogenic calcium carbonates in seawater, *Geochim. Cosmochim. Acta*, *44*, 241–252, 1980.

Lamb, M. F., et al., Consistency and synthesis of Pacific Ocean CO_2 survey data, *Deep Sea Res., Part II*, *49*, 21–58, 2002.

Lee, K., Global net community production estimated from the annual cycle of surface water total dissolved inorganic carbon, *Limnol. Oceanogr.*, *46*, 1287–1297, 2001.

Lee, K., F. J. Millero, and R. H. Wanninkhof, The carbon dioxide system in the Atlantic Ocean, *J. Geophys. Res.*, *102*, 15,693–15,707, 1997.

Lee, K., F. J. Millero, R. H. Byrne, R. A. Feely, and R. H. Wanninkhof, The recommended dissociation constants of carbonic acid for use in seawater, *Geophys. Res. Lett.*, *27*, 229–232, 2000.

Lee, K., et al., An undated anthropogenic CO_2 inventory in the Atlantic Ocean, *Global Biogeochem. Cycles*, submitted, 2003.

Lewis, E., and D. W. R. Wallace, Program developed for CO_2 system calculations, *Rep.105*, 33 pp., Carbon Dioxide Inf. Anal. Cent., Oak Ridge Natl. Lab., Oak Ridge, Tenn., Feb. 1998.

Lutz, M., R. Dunbar, and K. Caldeira, Regional variability in the vertical flux of particulate organic carbon in the ocean interior, *Global Biogeochem. Cycles*, *16*(2), 1037, doi:10.1029/2000GB001383, 2002.

Martin, W. R., and F. L. Sayles, $CaCO_3$ dissolution in sediments of the Ceara Rise, western equatorial Atlantic, *Geochim. Cosmochim. Acta*, *60*, 243–263, 1996.

Mehrbach, C., C. H. Culberson, J. E. Hawley, and R. M. Pytkowicz, Measurement of the apparent dissociation constants of carbonic acid in seawater at atmospheric pressure, *Limnol. Oceanogr.*, *18*, 897–907, 1973.

Millero, F. J., Influence of pressure on chemical processes in the sea, in *Chemical Oceanography*, 2nd ed., vol. 8, edited by J. P. Riley and R. Chester, chap. 43, pp. 2–88, Academic, San Diego, Calif., 1983.

Millero, F. J., Thermodynamics of the carbon dioxide system in the oceans, *Geochim. Cosmochim. Acta*, *59*, 661–677, 1995.

Millero, F. J., J.-Z. Zhang, K. Lee, and D. M. Campbell, Titration alkalinity of seawater, *Mar. Chem.*, *44*, 153–165, 1993.

Millero, F. J., K. Lee, and M. Roche, Distribution of alkalinity in the surface waters of the major oceans, *Mar. Chem.*, *60*, 111–130, 1998.

Milliman, J. D., and A. W. Droxler, Neritic and pelagic carbonate sedimentation in the marine environment: Ignorance is not bliss, *Geol. Rundsch.*, *85*, 496–504, 1996.

Milliman, J. D., P. J. Troy, W. M. Balch, A. K. Adams, Y.-H. Li, and F. T. Mackenzie, Biologically mediated dissolution of calcium carbonate above the chemical lysocline, *Deep Sea Res., Part I*, *46*, 1653–1669, 1999.

Morris, A. W., and J. P. Riley, The bromide/chemistry and sulfate/chlorinity ratio in seawater, *Deep Sea Res., Part I*, *13*, 699–705, 1966.

Morse, J. W., and R. A. Berner, Dissociation kinetics of calcium carbonate in seawater: II. A kinetic origin for the lysocline, *Am. J. Sci*, *272*, 840–851, 1972.

Morse, J. W., and F. T. Mackenzie, Geochemistry of sedimentary carbonates, 707 pp., Elsevier Sci., New York, 1990.

Mucci, A., The solubility of calcite and aragonite in seawater at various salinities, temperatures and 1 atmosphere total pressure, *Am. J. Sci.*, *238*, 780–799, 1983.

Pond, D. W., R. P. Harris, and C. A. Brownlee, Microinjection technique using a pH sensitive dye to determine the gut pH of Calanus helgolandicus, *Mar. Biol.*, *123*, 75–79, 1995.

Pytkowicz, R. M., Calcium carbonate retention in supersaturated seawater, *Am. J. Sci.*, *273*, 515–522, 1973.

Riley, J. P., The occurrence of anomalously high fluoride concentrations in the North Atlantic, *Deep Sea Res.*, *12*, 219–220, 1965.

Riley, J. P., and M. Tongudai, The major cation/chlorinity ratios in sea water, *Chem. Geol.*, *2*, 263–269, 1967.

Rubin, S., and R. M. Key, Separating natural and bomb-produced radiocarbon in the ocean: The potential alkalinity method, *Global Biogeochem. Cycles*, *16*(4), 1105, doi:10.1029/2001GB001432, 2002.

Sabine, C. L., F. T. Mackenzie, C. Winn, and D. M. Karl, Geochemistry of carbon dioxide in seawater at the Hawaii ocean time series station, *ALOHA, Global Biogeochem. Cycles*, *9*, 637–651, 1995.

Sabine, C. L., R. M. Key, R. A. Feely, and D. Greeley, Inorganic carbon in the Indian Ocean: Distribution and dissolution processes, *Global Biogeochem. Cycles*, *16*(4), 1067, doi:10.1029/2002GB001869, 2002a.

Sabine, C. L., R. A. Feely, R. M. Key, J. L. Bullister, F. J. Millero, K. Lee, T. H. Peng, B. Tilbrook, T. Ono, and C. S. Wong, Distribution of anthropogenic CO_2 in the Pacific Ocean, *Global Biogeochem. Cycles*, *16*(4), 1083, doi:10.1029/2001GB001639, 2002b.

Sarmiento, J. L., J. Dunne, A. Gnanadesikan, R. M. Key, K. Matsumoto, and R. Slater, A new estimate of the $CaCO_3$ to organic carbon export ratio, *Global Biogeochem. Cycles*, *16*(4), 1107, doi:10.1029/2002GB001919, 2002.

Sonnerup, R. E., On the relationships among CFC derived water mass ages, *Geophys. Res. Lett.*, *28*, 1739–1742, 2001.

Takahashi, T., Carbonate chemistry of seawater and the calcite compensation depth in the oceans: Special publication of the Cushman Foundation, *Foraminiferal Res.*, *13*, 11–126, 1975.

Uppström, L. R., Boron/chlorinity ratio of deep-sea water from the Pacific Ocean, *Deep Sea Res., Part I*, *21*, 161–162, 1974.

Walker, S. J., R. F. Weiss, and P. K. Salameh, Reconstructed histories of the annual mean atmospheric mole fractions for the halocarbons CFC-11, CFC-12, CFC-113, and carbon tetrachloride, *J. Geophys. Res.*, *105*, 14,285–14,296, 2000.

Wallace, D. W. R., P. Beining, and A. Putzka, Carbon tetrachloride and chlorofluorocarbons in the South Atlantic Ocean, 19°S, *J. Geophys. Res.*, *99*, 7803–7819, 1994.

Wanninkhof, R., T.-H. Peng, B. Huss, C. L. Sabine, and K. Lee, Comparison of inorganic carbon system parameters measured in the Atlantic Ocean from 1990 to 1998 and recommended adjustments, *ORNL/CDIAC-140*, 43 pp., Oak Ridge Natl. Lab., Oak Ridge, Tenn., 2003.

Warner, M. J., J. L. Bullister, D. P. Wisegarver, R. H. Gammon, and R. F. Weiss, Basin-wide distributions of chlorofluorocarbons CFC-11 and CFC-12 in the North Pacific: 1985–1989, *J. Geophys. Res.*, *101*, 20,525–20,542, 1996.

Yu, E.-F., R. Francois, M. P. Bacon, S. Honjo, A. P. Fleer, S. J. Manganini, M. M. Rutgers van der Loeff, and V. Ittekot, Trapping efficiency of bottom-tethered sediment traps estimated from the intercepted fluxes of ^{230}Th and ^{231}Pa, *Deep Sea Res., Part I*, *48*, 865–889, 2001.

Zondervan, I., R. E. Zeebe, B. Rost, and U. Riebesell, Decreasing marine biogenic calcification: A negative feedback on rising atmospheric pCO_2, *Global Biogeochem. Cycles*, *15*, 507–516, 2001.

J. L. Bullister, R. A. Feely, and C. L. Sabine, Pacific Marine Environmental Laboratory, NOAA, 7600 Sand Point Way, NE, Seattle, WA 98115-6349, USA. (3johnb@pmel.noaa.gov; feely@pmel.noaa.gov; sabine@pmel.noaa.gov)

S.-N. Chung and K. Lee (corresponding author), School of Environmental Science and Engineering, Pohang University of Science and Technology, San 31, Hyoja-dong, Nam-gu, Pohang, 790-784, Republic of Korea. (lady2592@postech.ac.kr; ktl@postech.ac.kr)

R. M. Key, Atmospheric and Oceanic Sciences Program, Princeton University, Forerstal Campus/Sayre Hall, Princeton, NJ 08544, USA. (key@princeton.edu)

F. J. Millero, Rosenstiel School of Marine and Atmospheric Studies, University of Miami, 4600 Rickenbacker Causeway, Miami, FL 33149, USA. (millero@rsmas.miami.edu)

T.-H. Peng and R. Wanninkhof, Atlantic Oceanographic and Meteorological Laboratory, NOAA, 4301 Rickenbacker Causeway, Miami, FL 33149, USA. (tsung-hung.peng@noaa.gov; rik.wanninkhof@noaa.gov)